Desalination and Water Treatment
www.deswater.com
doi: 10.5004/dwt.2019.24299

161 (2019) 283–292
September

Recycling of phosphorus from aqueous solutions by pine needles

Senay Balbay*

Department of Chemical Technologies, Vocational School, Bilecik Seyh Edebali University, 11230 Bilecik, Turkey, email: senay.balbay@bilecik.edu.tr

Received 13 December 2018; Accepted 17 April 2019

ABSTRACT

In this study, it is aimed to use phosphate ions in aqueous solution for production of phosphated organic fertilizers by using pine needles. Pine needles (PN), pine needles modified by NaOH (Na–MPN), pine needles modified by CH_3OH–NaOH solutions (MeOH–MPN) were used as adsorbents. Adsorbent amount (0.1–0.3 g/100 mL), contact time (15–1,440 min), pH (3–10), initial concentration (20–150 ppm) and temperature (25°C, 35°C, and 50°C) were the selected parameters. Microstructures, chemical and physical properties of the adsorbents were characterized, respectively, by Fourier transform infrared spectroscopy (PerkinElmer Spectrum 100, USA) and scanning electron microscope (ZEISS Supra 40VP, USA). According to experimental results and analyses, it was shown that lignin compound found in pine needles decreases the phosphate adsorption capacity of pine needles. The pseudo-second-order model for the Na–MPN adsorbent optimally fits the phosphate adsorption kinetics, and the data are coherent with Langmuir and Dubinin–Radushkevich (D-R) adsorption isotherm models. Furthermore, thermodynamic studies show that the adsorption process occurs spontaneously and naturally in an exothermic manner. As a result, it has been determined that it can be used as phosphated organic fertilizer in soils and waters where phosphate is insufficient by adsorbing phosphate ions to pine needles whose lignin were removed from waters having high phosphate concentration.

Keywords: Phosphate ion; Pine needles; Adsorption; Recycling

1. Introduction

Phosphorus is an important element for all living creatures in nature (humans, animals, microorganisms and plants). Phosphorus is most commonly used as a food additive in manure and animal feed. Besides, it is also used in foods, pharmaceuticals, detergents and some special chemicals [1].

Phosphorus in the environment is beneficial for many biological processes. However, the lack of phosphorus causes limited crop production in the soil, while too much phosphorus creates an imbalance in the ecosystem. Phosphorus concentration in nature is increasing due to the use of especially phosphorus-containing fertilizers, laundry detergents and pesticides [2].

There are three main ways in which phosphates are mixed into wastewater and groundwater: (1) separation from natural mineral deposits; (2) pesticides and fertilizers; (3) wastewater discharge and urban effluent (domestic and industrial). Due to the rapid growth of modern society, the amount of phosphorus released to nature increases day by day and accordingly, sewage water discharged into rivers, lakes and seas is in the form of phosphorus slurry [1].

Excess phosphate in water stimulates the growth of plankton and aquatic plants in favor of fast-growing species that have important roles in the ecosystem. In this

* Corresponding author.

phenomenon called eutrophication, overgrowth of plants consumes large amounts of dissolved oxygen which can suffocate fish. Moreover, excessive growth of the plants also prevents species living at the bottom from receiving sunlight. It causes short and long-term environmental and esthetic problems, eventually leading to the deterioration of water resources. In most countries, the phosphorus limit in water is 1–2 mg/L of total PO_4^{-3}–P [1,2].

Various techniques have been applied to remove phosphate from wastewater. Frequently used methods include chemical precipitation, biological processes and adsorption. Among them, adsorption is considered a reliable and effective technique for phosphate removal. Among these, adsorption is regarded as a reliable and an efficient technique in terms of phosphate removal. Both adsorption and recovery of phosphate can be done with the adsorption technique. An adsorption is a surface-based event resulting from the binding among the adsorbents due to covalent binding and electrostatic interactions [3].

The adsorption mechanism allows the adsorbent molecules to be absorbed through molecular interactions on the surface of the adsorbents and, and involves the separation of them from the surface of the adsorbate molecules to the surface of the adsorbent molecules in a single-layer or multi-layer manner. An adsorption event depends on various parameters such as the dosage, size and surface morphology of the adsorbent, the concentration and structure of the adsorbate, pH, temperature. In order to optimize the design of an adsorption system for the removal of P ions from aqueous solution, it is important to explain the relationship between adsorbed P ions per unit weight of adsorbent (q_e) and residual concentration of P ions in solution (C_e) at equilibrium. Important models such as Langmuir, Freundlich, Temkin, Dubinin–Radushkevich model, Redlich–Peterson, Harkins–Jura, Halsey, BET isotherm, intraparticle diffusion and Lagergren are used to explain the results of adsorption studies. Two kinetic models, that is, pseudo-first-order and pseudo-second-order models, are applied to determine the adsorption rate and mechanism of adsorption reactions. Thermodynamic parameters such as standard free energy change ($\Delta G°$), standard enthalpy change ($\Delta H°$) and standard entropy change ($\Delta S°$) are estimated to evaluate the feasibility of the adsorption process [4].

While selecting an adsorption method, both high capacity of adsorption and low cost are main issues that should be taken into consideration. Today, great importance is placed on low-cost adsorbents [5]. A great number of plant wastes have been used as adsorbents.

Pine needles are one among the plant wastes used as adsorbents. It was identified that there are K^+, Mg^{2+}, Ca^{2+}, SO_4^{2-} and PO_4^{-3} ions and phenolic compounds in pine needle extracts [6]. Researches have studied the removal of arsenic from the water by using pine needles. It was found that the adsorption mechanism followed second-stage kinetics. As a result of the study, it was concluded that pine needles could be a good adsorbent to remove As(V) from the water due to their excellent adsorption capacity [7]. Shepherd et al. [8] demonstrated that the recycling and reuse of phosphorus from the wastewater treatment systems as an agricultural fertilizer are significant and practicable for the reduction of P waste and its recycling. In their study, they developed novel biochar materials for the P adsorption from wastewater. In the biochars, plant accessibility of adsorbed P was taken into consideration. The results demonstrated that biochars could be potentially used as fertilizers [8].

Researchers predict that the need for the recovery and recycling of phosphate – being a non-renewable source that does not have known alternatives – may be necessary. Recycling of phosphorus from wastewater and redistribution to agricultural land is important to prevent phosphorus squander and scarcity [8]. In modern agriculture, dependence on mineral phosphorus fertilizers will increase much more if phosphorus released to nature is not recycled [1]. It is accepted that in the next 60 to 700 years, the phosphate reserves are all going to be consumed. Therefore, future studies should focus on the removal and recycling of PO_4^{-3} [3].

In this study, it is aimed to identify the phosphate ion adsorption capacity of pine needles from aqueous solutions and their potential usage for the production of organic phosphate fertilizers.

2. Experimental

2.1. Materials

Pine tree needles were obtained from the campus of Bilecik Seyh Edebali University in Turkey, and they were collected between February and March 2018. Analytical grade potassium phosphate monobasic (KH_2PO_4) obtained from Merck (Germany) was used as phosphate source in all experiments. Ammonium molybdate tetrahydrate ($(NH_4)_6Mo_7O_{24}{\cdot}4H_2O$), ammonium vanadate ($H_4NO_3V$) and nitric acid ($HNO_3$) purchased from Merck in Germany were used for phosphate analysis. NaOH and HCl chemicals were used to adjust the pH value. All other chemicals used in the study are of analytical grade.

2.2. Preparation of adsorbent

The pine needles (PN) were cut and repeatedly washed with distilled water to remove adhering dirt and soluble impurities. The pine needles modified by NaOH (Na–MPN) (10 g) were hydrolyzed with 100 mL solution of 1 M NaOH (to remove the lignin materials) at 80°C for overnight. The black solution (lignin) was removed by filtration. The solid phase was washed with distilled water until neutral pH = 7 was reached [9]. Modified pine needles by CH_3OH–NaOH solution (MeOH–MPN) (10 g) were hydrolyzed with 100 mL solution of 5% (w/v %) CH_3OH–NaOH solution (to remove the lignin) at 20°C overnight. The greenish solution (lignin) was removed by filtration. The solid phase was washed with distilled water until neutral pH = 7 was reached. All the washed adsorbents were dried in an oven at 50°C overnight. Finally, all the prepared adsorbents were kept in vacuum desiccators until the time of use.

2.3. Batch adsorption experiments

The phosphorus stock solution (250 mg/L) was prepared by dissolving 1.097 g of KH_2PO_4 in 1 L of distilled water. This solution was diluted to the desired concentrations.

Phosphorus was identified by finding out the adsorption characteristic wavelength using UV-spectrophotometer and vanadomolybdophosphoric acid colorimetric method. Under acidic conditions, phosphorus reacts with ammonium molybdate to form molybdo phosphoric acid. The resulting acid gives a yellow color with increasing concentrations of vanadium.

Reagents: Vanadomolybdate reagent (color enhancer) (A Solution + B solution + 70 mL of distillated water).

Solution A: 25 g of ammonium molybdate dissolved in 300 mL of water.

Solution B: 1.25 g ammonium metavanadate was dissolved by heating in 300 mL of water and after cooling, 330 mL of concentrated nitric acid was added.

Preparation of standard solutions: 10, 20, 40, 80, and 100 mg/L standard solutions were prepared from stock solution.

2 mL color enhancer and 7 mL of standard solution were added to 10 mL tubes. The remainder was then completed to 10 mL with distilled water [10].

The maximum absorbance (λ_{max} = 350 nm) values were determined by scanning absorbance of standard phosphorus solutions at different wavelengths (200–1,000 nm). A calibration graph was plotted using absorbance values against the concentration at a wavelength of 350 nm [11,12].

Preparation of Sample: 7 mL of sample, 2 mL of color enhancer and 1 mL of distilled water were added.

Adsorption kinetics was investigated by varying pH (3, 5, 7, and 10), contact times (15; 30; 60; 120; 360; 720; and 1,440 min) and adsorbent amount (0.1, 0.2, and 0.3 g/100 mL) with an initial phosphorus concentration of 50 mg/L at 20°C. Adsorption isotherms by varying the initial phosphorus concentrations (20, 50, 100, and 150 mg/L) and thermodynamic characteristics at the different temperatures (20°C, 35°C, and 50°C) were investigated. The adsorption experiments were conducted in 250 mL Erlenmeyer flasks that contained phosphorous solution at desired concentrations and adsorbent and they were stirred at 300 rpm at room temperature for 20°C ± 1°C. The effect of pH was investigated by varying the pH from 3.0 to 10.0 with 0.1 M NaOH and 0.1 M HCl solutions. Each experiment was repeated three times.

2.4. Analytical methods

Phosphorus concentration was measured by an ultraviolet–visible spectrophotometer through the TS 4082 method at 350 nm (JENWAY 7315, UK). The solution pH was measured by a standard pH meter (HANNA HI 991001, USA). The conductivity of solutions was determined by a standard conductivity pen (ULTRAPEN PT1). The morphological images of adsorbents were characterized by a scanning electron microscope (SEM-ZEISS Supra 40VP, USA). The functional group analyses of adsorbents were investigated using Fourier transform infrared spectroscopy (FT-IR; PerkinElmer, model spectrum 100, USA).

3. Results and discussion

The relationship between the conductivity and UV adsorption of phosphorus concentration is shown in Fig. 1. The conductivity of a solution depends on the ion concentration and ion types in the solution. Conductivity is a measure of ion concentration in the solution [13]. pH value gives H^+ ion concentration in the solution [14]. As the phosphorus concentration increases, pH was fixed approximately at 5. However, conductivity increased due to increased phosphorus concentration. Therefore, the hydrolysis of KH_2PO_4 actualized according to the reaction given below (Eq. (1)). Most of the phosphate ions are in the form of H_2PO_4 at 4–6 pH [15].

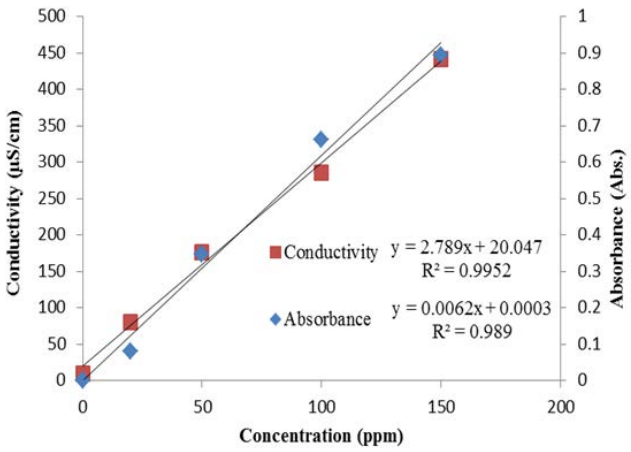

Fig. 1. Relationship between conductivity and UV absorbance of phosphorus concentration (*T*: 20°C).

$$KH_2PO_4 + H_2O \rightarrow K^+ + H_2PO_4^- + H_2O \quad (1)$$

3.1. Effect of pH

In order to identify the optimal pH value, the balance adsorption of the phosphate was carried out at 3–10 pH value, with adsorbent amount of 0.1 g/100 mL, with adsorption time of 24 h, at 20°C, by using 50 mg/L initial phosphate concentration. Most of the phosphate ions are found at different protonated forms at different pH values of the solution [15]. Main types of phosphorus in aqueous solution are H_3PO_4 at pH < ~4, $H_2PO_4^-$ at 4–6 pH, $H_2PO_4^-$ at pH = 7, HPO_4^{-2} at 9–11 pH, and PO_4^{-3} at pH > 11. Due to different negative charges between HPO_4^{2-} and H_2PO^{-4}, HPO_4^{-2} changes more hydroxyl compared with $H_2PO_4^-$ [16]. Positively charged adsorbent attracts the negatively charged ions. In this case, less protonated phosphate ions can be adsorbed more than the ones that have more protons. In this specific adsorption, the removal order of phosphate ions was PO_4^{-3} > HPO_4^{-2} > $H_2PO_4^-$ > H_3PO_4. Phosphate adsorption clearly showed that it strongly depended on the pH level of the solution. The highest removal of the phosphate occurred at 7 pH for PN and Na–MPN, and at 10 pH for M–MPN (Fig. 2). Accordingly, PN and Na–MPN were adsorbed as both $H_2PO_4^-$ and HPO_4^{-2} and MeOH–MPN were adsorbed as HPO_4^{-2}. It is possible for more hydrogen ions to be adsorbed on the surface from the solution at low pH levels (under 5 pH). Hence, an increase occurs at the ultimate pH of the solution [17]. In Fig. 3, where this incident is seen, the effect of solution pH on the phosphate adsorption is observed. It was observed that the pH of the solution remained approximately the same during

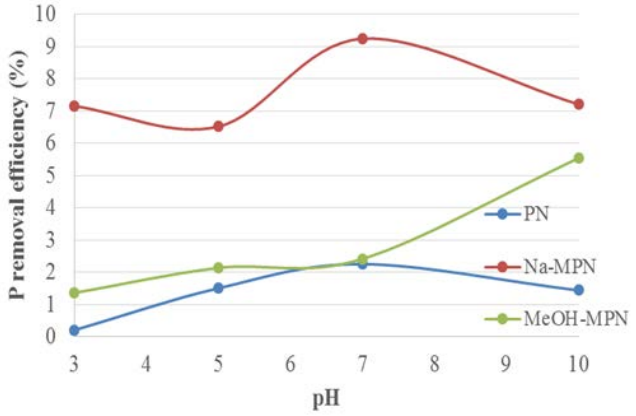

Fig. 2. Phosphate removal efficiency based on solution pH during phosphate adsorption on adsorbents (0.1 g/100 mL adsorbent amount, adsorption period of 24 h, and 50 mg/L initial phosphate concentration at 20°C).

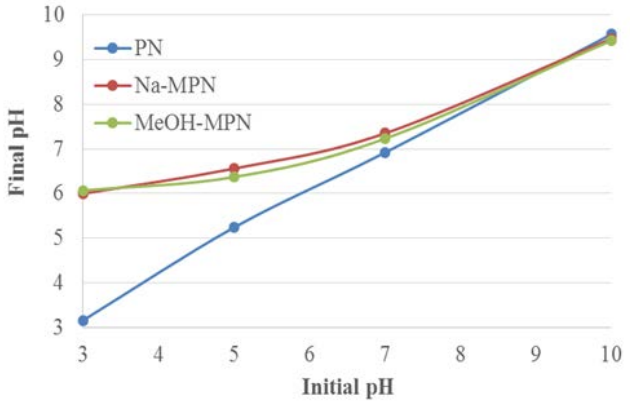

Fig. 3. Effect of solution pH during phosphate adsorption on adsorbents (0.1 g/100 mL adsorbent amount, adsorption period of 24 h, and 50 mg/L initial phosphate concentration at 20°C).

the adsorption period during the studies on contact time, adsorbent amount, initial concentration and temperature.

During the adsorption process, it is known that both pH and ionic strength are important factors [17]. During adsorption, the conductivity was measured in order to evaluate the extractability of ions by adsorbents. On the other hand, adsorbent solution and surface load play an important role in phosphate adsorption. At higher pH values, there is constant competition between hydroxylic ions (OH^-) and phosphate anions ($H_2PO_4^-$, HPO_4^{-2} and PO_4^{3}) for adsorption areas. Powerful hydroxyl ions may limit the approximation of phosphate anions as a result of repulsive force [17]. Depending on ion exchange reactions, a significant potassium ion increase occurred during the adsorption [18]. Due to these reasons, it was observed that the highest conductivity occurred at pH = 10 while the lowest conductivity occurred at pH = 5 (Fig. 4).

3.2. Effect of conductivity

The conductivity was measured in order to evaluate the extractability of ions by the adsorbents during the adsorption.

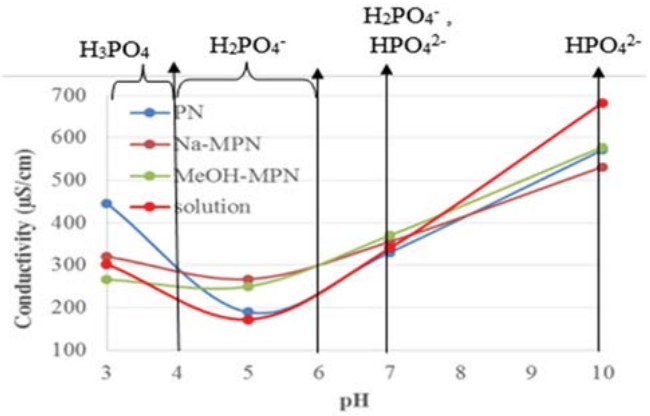

Fig. 4. Relationship between pH and conductivity during phosphate adsorption on adsorbents (0.1 g/100 mL adsorbent amount, adsorption period of 24 h, and 50 mg/L initial phosphate concentration at 20°C).

As it is shown in Fig. 5a, the conductivity did not change for PN and Na–MPN adsorbents. However, the conductivity increased up to 6 h for MeOH–MPN, and later it decreased. Due to the solvent effect of methyl alcohol, it is thought that especially the K^+, Mg^{2+}, Ca^{2+}, SO_4^{2-} and PO_4^{-3} ions included in the pine needles in MeOH–MPN adsorbent dispersed in the environment as they were dissolved in the solution up to 6 h; and they may have re-adsorbed on the adsorbent surface after 6 h.

For 0.1 g/100 mL adsorbent, with a contact time of 15 min at 20°C temperature in distilled water, the effect of adsorbents on conductivity was 325 µS/cm for PN, 330 µS/cm for Na–MPN and 445 µS/cm for MeOH–MPN. The conductivity of the solution did not differ significantly depending on the increasing amount of adsorbent (Fig. 5b).

The conductivity of the solution increased depending on the increasing initial concentration, and it was observed that the adsorbents in the phosphate solution increased the conductivity of the solution (Fig. 5c). This increase results due to the mixing of ions in the adsorbents into the solution as they are dissolved.

The conductivity did not significantly differ for PN and Na–MPN adsorbents according to the increasing temperature and the conductivity decreased for MeOH–MPN adsorbent (Fig. 5d).

3.3. Adsorption dynamics

Both the pseudo-first order model and pseudo-second-order model adsorption kinetics, which are among the commonly utilized kinetics models, were tested on the adsorbents in order to identify the optimal proportion for the adsorption of phosphate ions. Intraparticle diffusion model describes the adsorption rate depending on the diffusion rate [4]. Phosphate amount and concentration adsorbed by the adsorbents were calculated based on Eq. (2). Depending on time, until the first balance point of the reaction, they were analyzed with the pseudo-first-order model (Eq. (3)), the pseudo-second-order model (Eq. (4)) and the intraparticle diffusion model (Eq. (5)).

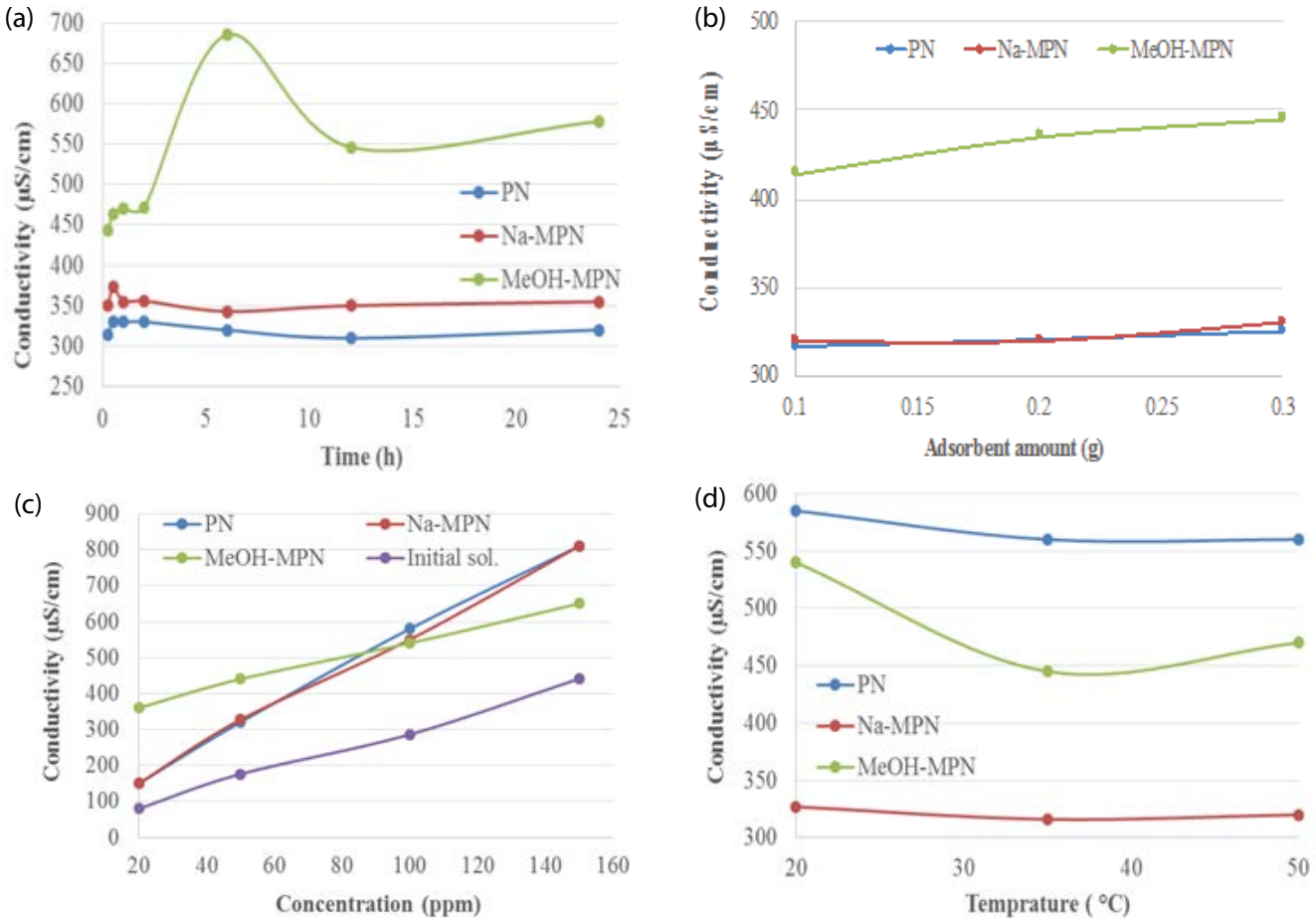

Fig. 5. Effect of phosphate adsorption on conductivity on adsorbents (a) right-top, (b) left-top, (c) right-bottom, and (d) left-bottom.

$$q_e = \frac{(C_0 - C_e)}{m} \times V \tag{2}$$

$$\ln(q_e - q_t) = \ln q_e - k_1 \times t \tag{3}$$

$$\frac{t}{q_t} = \frac{1}{k_2} \times q_e^2 + \frac{t}{q_e} \tag{4}$$

$$q_e = K_i \times t \,\hat{}\, 0.5 + C \tag{5}$$

C_0 (mg/L): initial concentration of phosphate solution, C_e (mg/L): the remaining phosphate concentration in the aqueous solution at equilibrium, V (L): volume of the solution, m(g): adsorbent amount, q_t and q_e (mg/g): adsorption capacity, respectively, at t moment and at equilibrium, k_1 and k_2: rate constants, respectively, for pseudo-first order model and pseudo-second-order model, t (min): time, K_i: the rate constant of the intraparticle transport (mg g^{-1} $min^{-0.5}$), C: the intercept.

The analysis results indicated that the adsorption kinetics do not match the pseudo-first order model; instead, it matches the pseudo-second-order model (Fig. 6). Due to the low correlation values obtained for all durations, intraparticle diffusion was formed (Fig. 7).

3.4. Identification of maximum adsorption capacity

The relationship between the adsorbed phosphate per adsorbent unit and phosphate concentration in the aqueous phase is graphically represented with adsorption isotherm. It shows how much phosphate can be distributed between liquid and solid phases at various equilibrium concentrations. The shape of the isotherm is determined by various

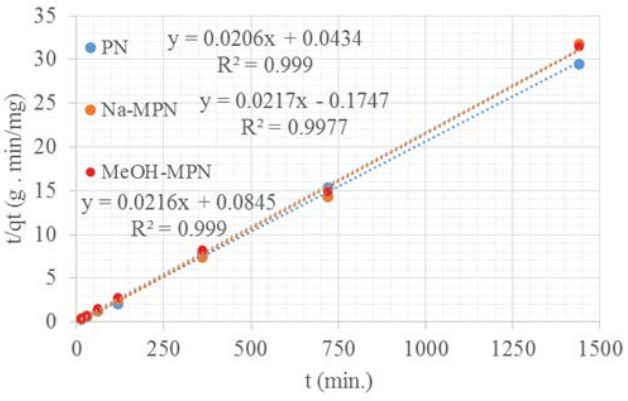

Fig. 6. Second stage model kinetics of phosphate adsorption on adsorbents.

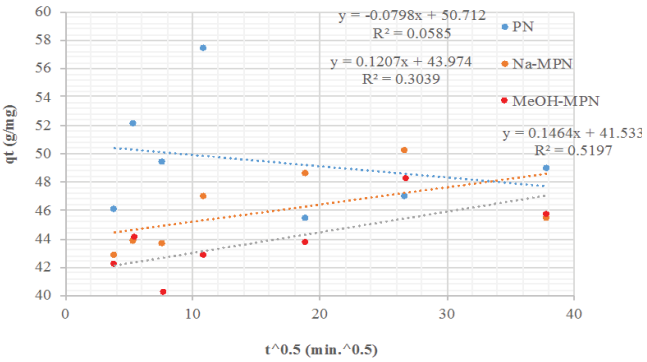

Fig. 7. Intraparticle diffusion model of phosphate adsorption on adsorbents.

factors such as the number of compounds in the solution, the initial concentration of compounds in the solution, their affinities for adsorption areas and the level of competition between solvents for active adsorption areas. Adsorption isotherm indicates to what extent the adsorption system is efficient and how efficient the adsorbate interacts with the adsorbent [9,18]. Isotherm analysis of adsorption process was examined in accordance with Langmuir and Freundlich isotherm models. According to the Langmuir isotherm model, adsorbent surface has a homogenous structure, and only one molecule can be adsorbed at each adsorption center and there is no interaction between the adsorbed molecules [19]. The Langmuir isotherm model is shown in Eq. (6). According to the Freundlich isotherm model, all the adsorption areas on the surface of an adsorbent have a heterogeneous structure [20]. The Freundlich isotherm model is shown in Eq. (7). The Temkin isotherm is usually used for heterogeneous surface energy systems (non-uniform distribution of adsorption heat) [21]. The Temkin isotherm model is shown in Eq. (8). The Dubinin–Radushkevich (D-R) isotherm model is used to estimate the characteristic porosity and the apparent free energy of adsorption [4]. The D-R isotherm model is given in Eq. (9) as follows:

$$\frac{C_e}{q_e} = \frac{C_e}{q_{\max}} + \frac{1}{K_L \times q_{\max}} \tag{6}$$

$$\ln q_e = \ln K_f + \frac{\ln C_e}{n} \tag{7}$$

$$q_e = \frac{RT}{b} \ln A + \frac{RT}{b} \ln C_e \tag{8}$$

$$\ln q_e = \ln q_m - \beta\varepsilon^2 \tag{9}$$

q_e: amount of P per unit mass of adsorbate (mg/g), C_e: equilibrium concentration (mg/L), $q_{\max}$: maximum theoretical phosphate adsorption capacity (mg/g), K_L: Langmuir affinity constant (L/mg), K_f and n: Freundlich constants, A (slope): Temkin isotherm equilibrium binding constant (L/g), b (intercept): Temkin isotherm constant, R: universal gas constant (8.314 J/mol/K), T: Temperature (K), ε: the polanyi potential, q_m: the monolayer capacity (mol/g), β: the D–R model constant (J/mol).

Langmuir, Freundlich, Temkin, Dubinin–Radushkevich isotherms and intraparticle diffusion model correlation coefficients of phosphate adsorption on adsorbents were given in Table 1. When the correlation coefficients of all models for Na–MPN adsorbent are compared, it can be seen that the phosphate adsorption process on adsorbent surface is more compatible with Langmuir and D-R models (D-R $R^2 = 0.99 \geq$ Langmuir $R^2 = 0.98 >$ Freundlich $R^2 = 0.89$). Moreover, the compatibility with the D-R isotherm indicates that the surface of the adsorbent is not fully homogeneous. As it is evidenced by correlation coefficient R^2, it is evident that the entire adsorption isotherm of phosphate can be described better by using Langmuir model compared with Freundlich. These results suggest that the phosphate has a single layer cover on its adsorbent surface which is not fully homogeneous. The other adsorption isotherms are not appropriate for Na–MPN adsorbent. Furthermore, when the correlation coefficients of both models are compared for PN and MeOH–MPN, it is seen that the former is more compatible with Langmuir model (Langmuir $R^2 = 0.39 >$ Freundlich $R^2 = 0.06$) while the latter is more compatible with Freundlich model (Langmuir $R^2 = 0.44 <$ Freundlich $R^2 = 0.60$) (Figs. 8–11). All the adsorption isotherms are not appropriate for PN and MeOH–MPN adsorbent.

Shafique et al. [7] studied the adsorption of As^{+5} (pentavalent arsenic) onto pine leaves. The order of fit in relation to coefficient of correlation was Langmuir > Freundlich > Dubinin–Radushkevich > Temkin. The interaction between adsorbate and adsorbent was second-order kinetics [7]. The results of this study are similar to our study due to Langmuir isotherm and second-order kinetics results. It was concluded that the pine needles can be an excellent adsorbent for removing toxic As(V) and phosphorus ions from water.

3.5. Thermodynamic parameters

Gibbs free energy change of adsorption process (ΔG°) is related to the equilibrium constant of classic Van't Hoff

Table 1
Langmuir, Freundlich, Temkin and Dubinin–Radushkevich isotherms correlation coefficients of phosphate adsorption on adsorbents

	R^2			
	Langmuir	Freundlich	Temkin	Dubinin–Radushkevich
PN	0.3979	0.0679	0.8175	0.0263
MeOH–MPN	0.4498	0.6015	0.1277	0.0861
Na–MPN	0.9879	0.8948	0.7324	0.9926

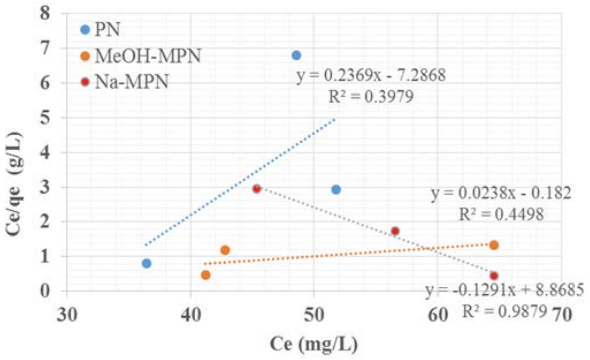

Fig. 8. Langmuir isotherm model of phosphate adsorption on adsorbents (equilibration time: 15 min, *T*: 20°C for PN, Na–MPN and MeOH–MPN, and pH: 7, 0.3 g/100 mL for PN, and pH: 7, 0.1 g/100 mL for Na–MPN, and pH: 10, 0.3 g/100 mL for MeOH–MPN).

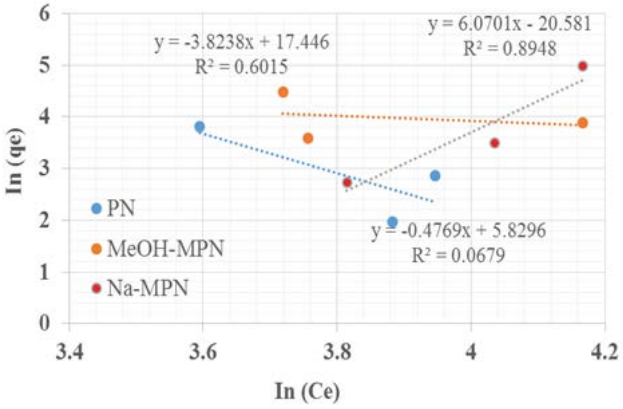

Fig. 9. Freundlich isotherm model of phosphate adsorption on adsorbents (equilibration time: 15 min, *T*: 20°C for PN, Na–MPN and MeOH–MPN, and pH: 7, 0.3 g/100 mL for PN and pH: 7, 0.1 g/100 mL for Na–MPN, and pH: 10, 0.3 g/100 mL for MeOH–MPN).

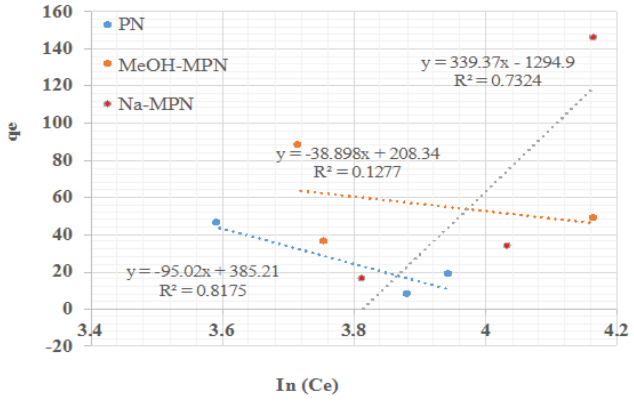

Fig. 10. Temkin isotherm model of phosphate adsorption on adsorbents (equilibration time:15 min, *T*: 20°C for PN, Na–MPN and MeOH–MPN, and pH: 7, 0.3 g/100 mL for PN, and pH: 7, 0.1 g/100 mL for Na–MPN, and pH: 10, 0.3 g/100 mL for MeOH–MPN).

equation (Eq. (10)). According to thermodynamics, Gibbs free energy change is related to entropy change in constant temperature ($\Delta S°$) and adsorption heat ($\Delta H°$) (Eq. (11)).

$$\Delta G° = -RT \ln K_d \tag{10}$$

$$\ln K_d = \frac{\Delta S°}{R} - \frac{\Delta H°}{RT} \tag{11}$$

T is absolute temperature (K) and *R* is ideal gas constant (8.314 J/mol*K). $\Delta S°$ and $\Delta H°$ were calculated by drawing 1/*T* graph against ln K_d by the help of Van't Hoff curve (Fig. 12). For PN, Na–MPN, and MeOH–MPN adsorbents, the $\Delta S°$(kJ/mol) values were, respectively, 0.132, 0.072 and 0.034; $\Delta H°$(kJ/mol) values were, respectively, –46.2, –28.32 and –13.6; and $\Delta G°$(kJ/mol) values for 303 K were calculated as –86.2, –50.14 and –23.9, respectively. Acquired negative $\Delta G°$ values indicated that these were thermodynamically appropriate and the phosphate adsorption occurred autogenously. Positive $\Delta S°$ values reflect the affinity of surface active substance modified adsorbents to phosphate adsorption, and negative $\Delta H°$ shows the exothermic nature

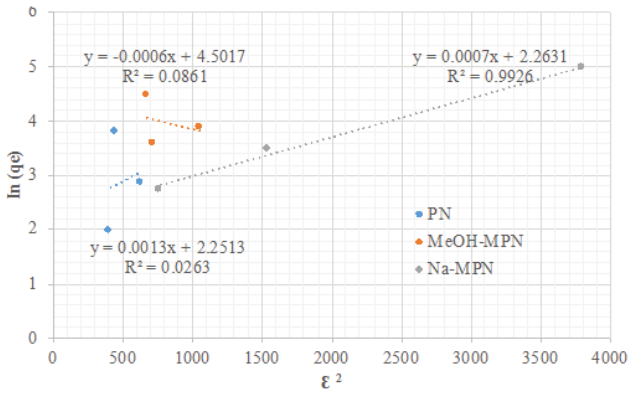

Fig. 11. Dubinin–Radushkevich model of phosphate adsorption on adsorbents (Equilibration time:15 min, *T*: 20°C for PN, Na–MPN and MeOH–MPN, and pH: 7, 0.3 g/100 mL for PN, and pH: 7, 0.1 g/100 mL for Na–MPN, and pH: 10, 0.3 g/100 mL for MeOH–MPN).

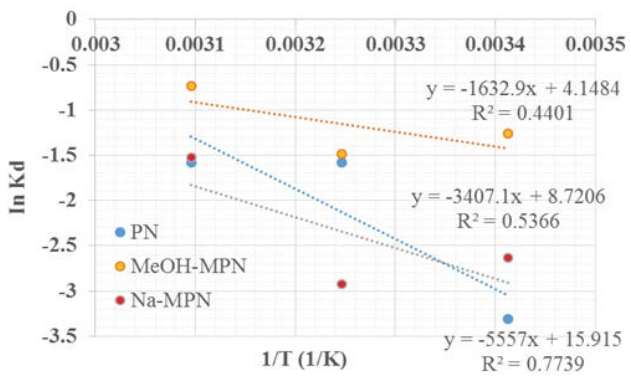

Fig. 12. lnK_d – 1/*T* graph for the estimation of thermodynamic parameters for phosphate adsorption on adsorbents.

of the adsorption process. Positive entropy change values also indicate that the randomness increased at solid/solution interface during the adsorption process.

FT-IR and SEM analyses of each adsorbent of which the optimal working conditions were identified were conducted both before and after the adsorption.

3.6. FT-IR analysis of adsorbents

FT-IR spectrums of adsorbents for both before and after adsorption are given in Fig. 10. Strong adsorption peak seen at around 150/cm was ascribed to P–O asymmetric tension vibration peak on adsorbent after phosphate adsorption [22]. Similar to the study of Tu et al. [22], it was seen that PO_4^{-3} adsorbed on Na–MPN after adsorption for Na–MPN. On the other hand, O–H vibration peak observed at around 3,320/cm wavelength for Na–MPN was not seen after the adsorption. $H_2PO_4^-$ and HPO_4^{-2} forms adsorbed on the adsorbent surface by bonding with hydroxyl ions in the adsorbent. Bands, respectively, observed at ~2,930; 2,900–2,850; and 1,710/cm result from the aromatic C–H, aliphatic (–CH–) and C=O stretching in the structure of lignin [23]. As the aromatic C–H, aliphatic (–CH) bonds observed in Na–MPN adsorbent at the vibration peaks of ~2,930; 2,900–2,850; and 1,710/cm bonded with $H_2PO_4^-$, HPO_4^{-2} ions, these peaks clearly decreased for Na–MPN adsorbent after adsorption (Fig. 13). It was observed that the sharp lignin peaks seen for PN and MeOH–MPN adsorbents remained the same as sharp and narrow after the adsorption and did

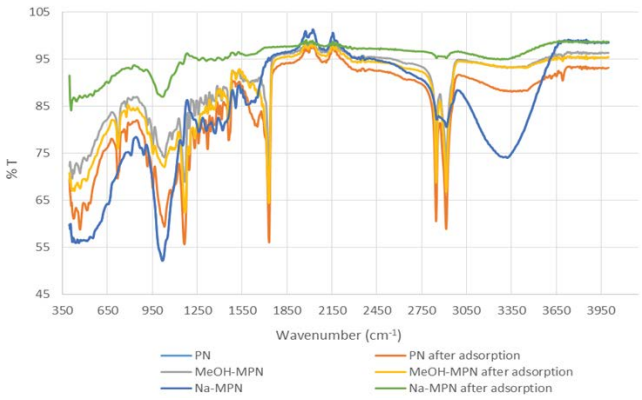

Fig. 13. FT-IR patterns of absorbances before and after adsorption phosphate.

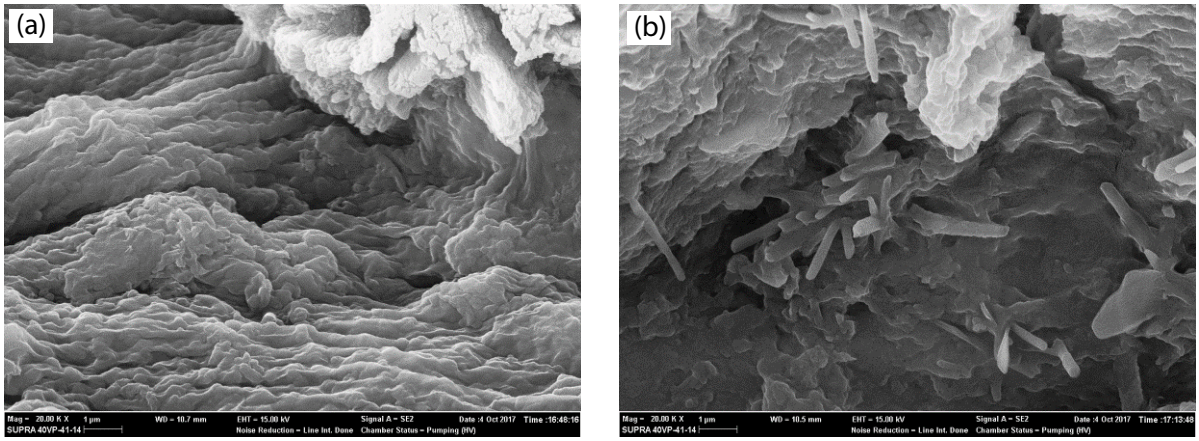

Fig. 14. SEM images of Na–MPN (a) before adsorption and Na–MPN (b) after adsorption (20.000×).

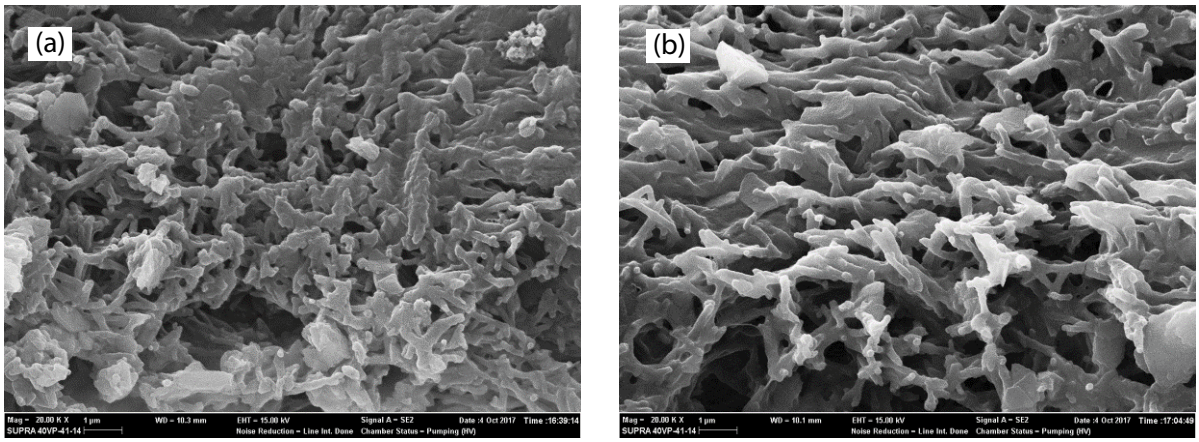

Fig. 15. SEM images of PN (a) before adsorption and PN (b) after adsorption (20.000×).

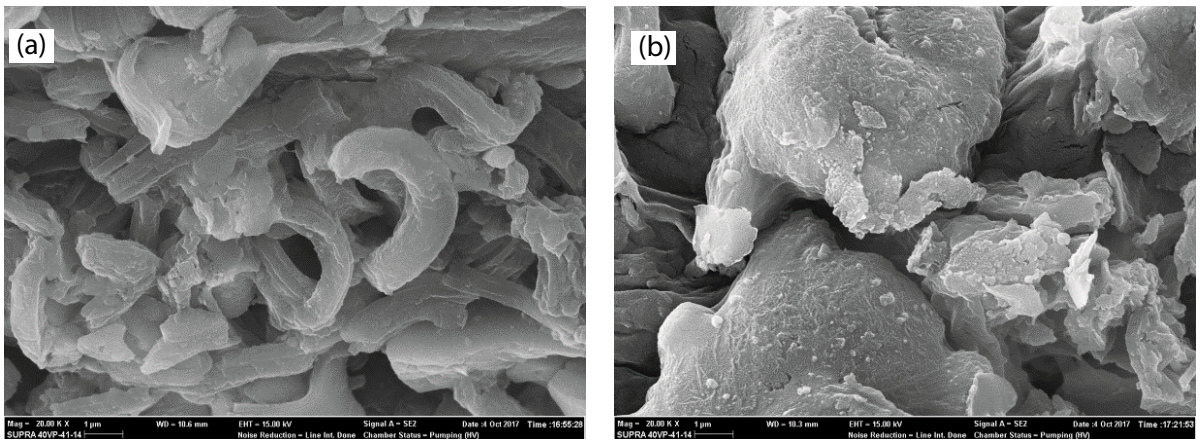

Fig. 16. SEM images of MeOH–MPN (a) before adsorption and MeOH–MPN and (b) after adsorption (20.000×).

not change. It was seen that the phosphate ions were not able to sufficiently adsorb on the adsorbent surface due to the C=O bond on the structures of PN and MeOH–MPN adsorbents.

3.7. SEM images of adsorbents

SEM images of adsorbents before and after the adsorption are given in Figs. 14–16. While it can be clearly seen that the phosphate ions adsorbed as a bar for Na–MPN adsorbent, it was observed that PN and MeOH–MPN adsorbents did not adsorb on the surface and they only formed a residue.

4. Conclusion

In the study, identifying the adsorption capacity of pine needles on phosphate ions in aqueous solutions, the evaluations of both pine needles and phosphate ions in aqueous solution have been examined. Phosphate adsorption has clearly shown that it strongly depends on the pH level of the solution. The highest removal of the phosphate occurred at 7 pH for PN and Na–MPN, and at 10 pH for M–MPN. Accordingly, both PN and Na–MPN were adsorbed as $H_2PO_4^-$ and HPO_4^{-2} and MeOH–MPN was adsorbed as HPO_4^{-2}. Depending on ion exchange reactions, a significant potassium ion increase occurred during the adsorption. Due to these reasons, it was observed that the highest conductivity occurred at pH = 10 while the lowest conductivity occurred at pH = 5. The analysis results indicated that the adsorption kinetics matches the pseudo-second-order model. Due to the low correlation values obtained for all durations, intraparticle diffusion was formed. When the correlation coefficients of all models for Na–MPN adsorbent are compared, it can be seen that the phosphate adsorption process on adsorbent surface is more compatible with Langmuir and D-R models. All the adsorption isotherms are not appropriate for PN and MeOH–MPN adsorbent. Furthermore, thermodynamic studies show that the adsorption process autogenously occurs in nature in an exothermic manner. It was observed that the sharp lignin peaks seen for PN and MeOH–MPN adsorbents remained sharp and same after the adsorption and did not change. It was seen that the phosphate ions were not able to sufficiently adsorb on the adsorbent surface due to the C=O bond on the structures of PN and MeOH–MPN adsorbents.

These results indicate that the pine needles from which the lignin is removed have a significant potential for removing phosphate from wastewater that contains high phosphate. Furthermore, it is concluded that the phosphate in the wastewater can be collected from the environment with this method, and it can be used as an organic phosphate fertilizer in soils and water where the phosphate is insufficient.

Acknowledgments

The author would like to acknowledge the author's student Emre Poyraz for their kind help and assistance.

References

[1] O. Panasiuk, Phosphorus Removal and Recovery from Wastewater using Magnetite, Royal Institute of Technology, M.Sc. Thesis, Stockholm, 2010.
[2] T. Phesatcha, S. Tukkeeree, J. Rohrer, Determination of Total Phosphorus in Wastewater Using Caro's Reagent and Ion Chromatography, Thermo Fisher Scientific Inc., 2016, Available at: https://assets.thermofisher.com/TFS-Assets/CMD/Application-Notes/AN-254-IC-Total-Phosphorus-Wastewater-AN71350-EN.pdf.
[3] J. Lalley, C. Han, X. Li, D.D. Dionysiou, M.N. Nadagouda, Phosphate adsorption using modified iron oxide-based sorbents in lake water: kinetics, equilibrium, and column tests, Chem. Eng. J., 284 (2016) 1386–1396.
[4] R. Bushra, A. Ahmed, M. Shahadat, Mechanism of Adsorption on Nanomaterials, C.M. Hussain, B. Kharisov Eds., Advanced Environmental Analysis: Applications of Nanomaterials, Vol. 1, Chapter 5, The Royal Society of Chemistry, 2017, Available at: https://doi.org/10.1039/9781782623625-00090.
[5] X. Yuan, W. Xia, J. An, J. Yin, X. Zhou, W. Yang, Kinetic and thermodynamic studies on the phosphate adsorption removal by dolomite mineral, Hindawi Publ. Corp. J. Chem., 2015 (2015) 8 p.
[6] J.S. Hwang, J.J. Bae, Y.S. Choo, Effects of an aqueous red pine (Pinus densiflora) needle extract on growth and physiological characteristics of soybean (Glycine max), J. Ecol. Field Biol., 34 (2011) 279–286.
[7] U. Shafique, A. Ijaz, M. Salman, W. uz Zaman, N. Jamil, R. Rehman, A. Javaid, Removal of arsenic from water using pine leaves, J. Taiwan Inst. Chem. Eng., 43 (2012) 256–263.

[8] J.G. Shepherd, S.P. Sohi, K.V. Heal, Optimising the recovery and re-use of phosphorus from wastewater effluent for sustainable fertiliser development, Water Res., 94 (2016) 155–165.
[9] S. Debnath, N. Ballav, A. Maity, K. Pillay, Competitive adsorption of ternary dye mixture using pine cone powder modified with β-cyclodextrin, J. Mol. Liq., 225 (2017) 679–688.
[10] TS 4082 EN 1189, Water Quality – Determination of Phosphorus – Ammonium molybdate Spectrometric method.
[11] Food and Nutrition Board, Food Chemicals Codex, 3rd ed., The National Academies Press, Washingtion, D.C., 1981.
[12] J.W. Williams, Handbook of Anion Determitaion, Butterworths, 1984.
[13] H. Yalçın, M. Gürü, Water Technology, 1st ed., Palme Publications, Ankara, Turkey, 2012.
[14] F. Şengül, A. Müezzinoğlu, Water Chemistry, Dokuz Eylül University ed., İzmir, Turkey, 2001.
[15] A. Sreenivasulu, E.V. Sundaram, M.K. Reddy, Phosphate adsorption studies using carbon prepared from stem bark of *Eucalyptus teriticornis* Smith, Indian J. Chem. Technol., 6 (1999) 256–262.
[16] M. Pan, X. Lin, J. Xie, X. Huang, Kinetic, equilibrium and thermodynamic studies for phosphate adsorption on aluminum hydroxide modified palygorskite nano-composites, RSC Adv., 7 (2017) 4492.
[17] Y.-J. Tu, C.-F. You, C.-K. Chang, M.-H. Chen, Application of magnetic nano-particles for phosphorus removal/recovery in aqueous solution, J. Taiwan Inst. Chem. Eng., 46 (2015) 148–154.
[18] B.S. Chittoo, C. Sutherland, Adsorption of phosphorus using water treatment sludge, J. Appl. Sci., 14 (2014) 3455–3463.
[19] I. Langmuir, The adsorption of gases on plane surfaces of glass, mica and platinum, J. Am. Chem. Soc., 40 (1918) 1361–1403.
[20] H. Freundlich, Über die adsorption in lösungen, Ind. Eng. Chem. Fundam., 57 (1906) 385–470.
[21] M. Erhayem, F. Al-Tohami, R. Mohamed, K. Ahmida, Isotherm, kinetic and thermodynamic studies for the sorption of mercury (II) onto activated carbon from *Rosmarinus officinalis* leaves, Am. J. Anal. Chem., 6 (2015) 1–10.
[22] C. Tu, S. Wang, W. Qiu, R. Xie, B. Hu, G. Qu, P. Ning, Phosphorus removal from aqueous solution by adsorption onto La-modified clinoptilolite, MATEC Web Conf., International Symposium on Materials Application and Engineering, 67 (2016) 14 p.
[23] C.G. Boeriu, D. Bravo, R.J.A. Gosselink, J.E.G. van Dam, Characterisation of structure-dependent functional properties of lignin with infrared spectroscopy, Ind. Crops Prod., 20 (2004) 205–218.